openDD: A Large-Scale Roundabout Drone Dataset

Antonia Breuer[1], Jan-Aike Termöhlen[2], Silviu Homoceanu[1], Tim Fingscheidt[2]

***Abstract*— Analyzing and predicting the traffic scene around the ego vehicle has been one of the key challenges in autonomous driving. Datasets including the trajectories of all road users present in a scene, as well as the underlying road topology are invaluable to analyze the behavior of the various traffic participants. The interaction between the traffic participants is especially high in intersection types that are not regulated by traffic lights, the most common one being the roundabout. We introduce the `openDD` dataset, including 84,774 accurately-tracked trajectories and HD map data of seven different roundabouts. The `openDD` dataset is annotated using images taken by a drone in 501 separate flights, totalling in over 62 hours of trajectory data. As of today the `openDD` is by far the largest publicly available trajectory dataset recorded from a drone perspective, while comparable datasets span 17 hours at most. The data is available, for both commercial and non-commercial use, at: `http://www.l3pilot.eu/openDD`.**

I. INTRODUCTION

In recent years autonomous driving has become one of the major applications for numerous fields of research. A main challenge faced in autonomous driving is the prediction of the traffic scene surrounding the ego vehicle. Predicting the surrounding traffic scene is particularly difficult in urban and rural scenarios due to the high inter-dependency between the involved road users. One way to face this challenge is to use increasing amounts of data, causing a surge of popularity of data-driven approaches that rely on large-scale datasets in recent years [1], [2], [3], [4]. Other applications of trajectory datasets include the modeling and analysis of driving behavior [5] and the analysis of safety of the autonomous driving function [6].

Datasets recorded from a ground view instead of a bird's eye perspective are limited by occlusions and the restricted field of view of the recording device at the ground. Labeling the trajectories with the help of image data captured by an aerial drone ensures a complete overview of the traffic situation and enables algorithms that use the dataset to take all present road users into account. The interaction between different road users is particularly high in intersections that are not regulated by traffic lights, the most common being the roundabout. In the `openDD` dataset presented in this work, seven roundabouts with different topologies are covered, one of them shown in Fig. 1. The dataset includes trajectories of all recorded road users, shapefiles and an extensible markup language (XML) file, describing the road topology of the underlying intersections. One reference image taken by the drone is provided per intersection. An exemplary visualization of the data included in the dataset can be seen in Fig. 1. As shown there, all dynamic traffic participants are accurately tracked in the relevant area surrounding the roundabout, and also vehicles hard to see for the human eye, such as the grey car on top of the picture are accurately detected. The introduced `openDD` dataset spans more than 62 hours in total, covers $84,774$ trajectories, and can be accessed on the following website: `http://www.l3pilot.eu/openDD`.

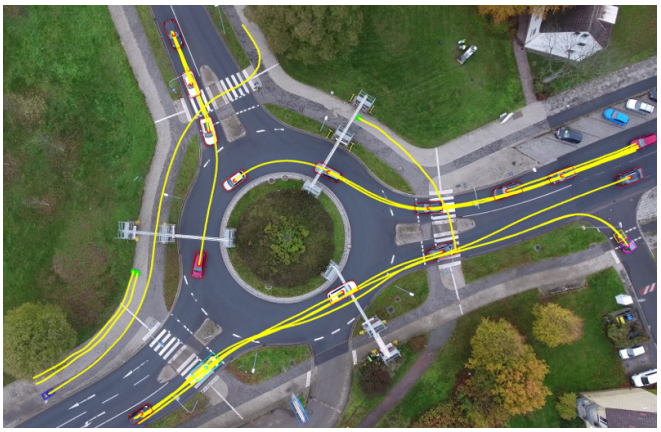

Fig. 1: An exemplary visualization of a given traffic scene included in the dataset. The past trajectories of all present objects relative to the given time instant n are drawn in yellow. The bounding box of object j is depicted in the color corresponding to its class $c_n^{(j)}$.

II. RELATED WORK

Table I gives an overview of trajectory datasets recorded from a drone perspective and their characteristics.

The `Stanford drone` dataset [7] was the first publicly available trajectory dataset recorded from a drone's perspective and is tailored to the analysis of pedestrian trajectories. It consists of 9 hours of data over eight unique locations on the campus and has a high percentage rate of labeled pedestrians and cyclists, while only about 7% of the labeled targets are cars. The `DUT` and `CITR` datasets [9] are especially designed for the analysis of the behavior of pedestrians when interacting with vehicles and span less than half an hour in total. One of the first large-scale trajectory datasets based on the footage of an aerial drone is the `highD` dataset [8]. It includes trajectory data from $110,000$ cars on German highways and spans $5,600$ lane changes over 16.5 hours of data. During the creation of the presented `openDD` dataset, descriptions

[1]Antonia Breuer and Silviu Homoceanu are with Volkswagen, Berliner Ring 2, 38440 Wolfsburg, Germany. {`antonia.breuer, silviu.homoceanu`}`@volkswagen.de`

[2]Jan-Aike Termöhlen and Tim Fingscheidt are with the Institute for Communications Technology, Technische Universität Braunschweig, Schleinitzstr. 22, 38106 Braunschweig, Germany. `j.termoehlen, t.fingscheidt@tu-bs.de`

TABLE I: Overview of trajectory datasets recorded by a drone published in recent years.

Dataset Name	Length	Situations	# locations	# trajectories	Map	Classes	License
Stanford Drone [7]	9.00 h	campus	8	10,240	none	pedestrians, bicycles, cars, skateboards, carts, buses	non-commercial
highD [8]	16.50 h	highway	6	110,000	none	cars, trucks	non-commercial
CITR [9]	0.21 h	parking lot	1	340	none	pedestrians	non-commercial
DUT [9]	0.16 h	urban intersections, shared space	2	1,793	none	pedestrians	non-commercial
inD [10]	10.00 h	urban intersections	4	11,500	none	pedestrians, bicycles, cars, trucks, buses	non-commerical
INTERACTION [11]	16.50 h	urban intersections, highway	11	40,054	lanelet2 [12]	cars, pedestrians	non-commerical
openDD	62.70 h	roundabouts	7	84,774	shapefiles	cars, vans, trucks, buses, pedestrians, trailers, motorcycles, bicyclists	non-commerical & commercial

of the INTERACTION [11] and the inD [10] datasets have been published. The INTERACTION dataset spans about 16.5 hours and covers data from 11 intersections, including 5 roundabouts, 3 unsignalized intersections, 2 merging and lane change situations, and 1 signalized intersection. The InD dataset [10] distinguishes pedestrians, bicycles, cars, trucks, and buses and includes 10 hours of data recorded by a drone. At the time of writing of this publication, the InD dataset has not been released yet, thus no further description than the one stated in the publication can be given.

III. DATASET

This work introduces the openDD dataset, a trajectory dataset recorded from a drone perspective. The dataset includes $R = 501$ recordings, each representing one coherent drone flight, capturing one of the $I = 7$ roundabouts covered in the dataset, depicted in Fig. 2. Each recording indexed by $r \in \mathcal{R} = \{1, \dots, R\}$ spans 5 to 15 minutes in total and was taken from the drone perspective with a camera capturing 30 fps. The used drone is a DJI Phantom 4, a high-end consumer drone, recording at a resolution of 3840×2160 pixels, being slightly below 4K. The video footage taken by the drone is stabilized and rectified before it is used to detect and track all traffic participants in the given scene.

For each recording r we define N_r to be the number of time instants included in the recording, equal to the number of frames captured in the recorded video.

The openDD dataset defines which objects, each with unique object index j are present at time instant $n \in \{1, \dots, N_r\}$. The state vector $\mathbf{s}_n^{(j)}$ of an object j at a time instant n is defined by ($[]^T$ being the transpose)

$$\begin{aligned}\mathbf{s}_n^{(j)} = [&x_n^{(j)}, \quad y_n^{(j)}, \quad \alpha_n^{(j)}, \quad w_n^{(j)}, \quad l_n^{(j)}, \\ &v_n^{(j)}, \quad a_{\mathbf{l},n}^{(j)}, \quad a_{\mathbf{t},n}^{(j)}, \quad a_n^{(j)}, \quad c_n^{(j)}]^T.\end{aligned} \tag{1}$$

The vector $\left[x_n^{(j)}, y_n^{(j)}\right]^T$ describes the Universal Transverse Mercator (UTM) coordinates of the object's bounding box center. The orientation of the bounding box is given by its yaw $\alpha_n^{(j)}$ in radiants relative to the x-axis of the UTM reference coordinate system, whereas the dimension of the bounding box is given by the width $w_n^{(j)}$ and length $l_n^{(j)}$. The dynamic state of the object is described by the velocity $v_n^{(j)}$ defined in $\mathrm{m/s}$, whereas $a_{\mathbf{l},n}^{(j)}$, $a_{\mathbf{t},n}^{(j)}$, and $a_n^{(j)}$ describe the **l**ateral, **t**angential, and total acceleration of the object in $\mathrm{m/s^2}$. Additionally, the class $c_n^{(j)} \in \mathcal{C} = \{C, V, T, B, P, R, M, Y\}$ of the object is defined, with each object either being a passenger **c**ar, **v**an, **t**ruck, **b**us, **p**edestrian, t**r**ailer, **m**otorcycle, or bic**y**clist. A visualization of the included bounding box information and the color-encoded class labels for a given scene can be seen in Fig. 1.

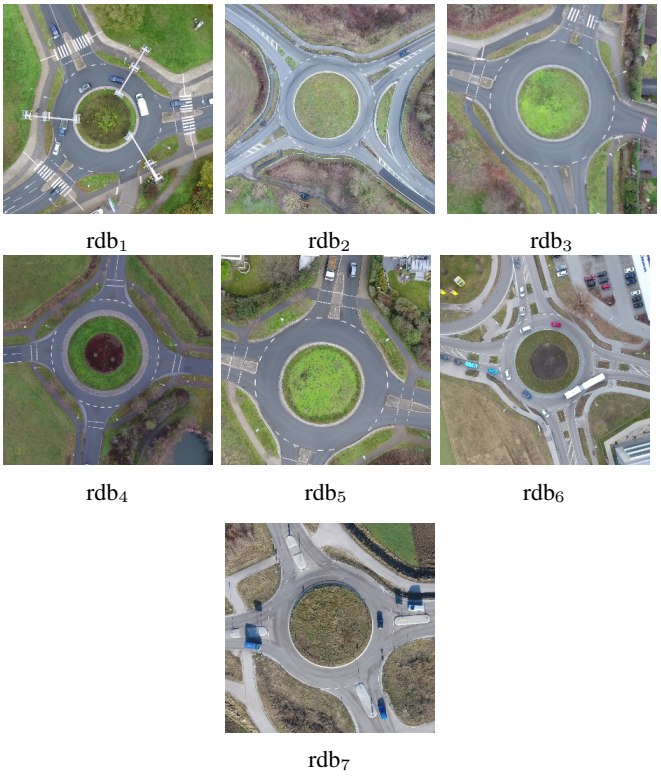

Fig. 2: An overview of the seven roundabouts included in the openDD dataset, with their respective abbreviation rdb_i used in the dataset, $i \in \{1, 2, \dots, 7\}$.

We provide the underlying HD map for each roundabout rdb_i with $i \in \{1, \dots, I\}$ included in the dataset. The map data is provided as shapefiles and an XML file and distinguishes three logical elements of the road topology:

lane centerlines, lane boundaries, and drivable areas. For each such logical element, three shapefiles are provided, a `.shp`, a `.shx`, and a `.dbf`, resulting in a total of nine shapefiles included in the dataset per roundabout. The `.shp` file defines the underlying geometry of the logical element, such as the points of the lanes. The `.dbf` attribute files are in `dBase` format and define element-specific attributes. For the lane centerlines, the `.dbf` file contains, among other attributes, a unique identifier for each lane centerline and a list of succeeding lane centerlines, preceding lane centerlines, and parallel lane centerlines. The `.dbf` file for the lane boundaries defines the corresponding lane identifier, as well as the material of the lane boundary, such as `CONCRETE` for a curbstone and `NONE` for an implicit lane boundary. The `.shx` file is an index file of the shape geometry `.shp` file, providing a way to quickly iterate over the defined geometry. An exemplary visualisation of the provided shapefiles is given in Fig. 3. In addition to the shapefiles we also provide an `.XML` file for each intersection i, representing the information contained in the shapefiles in a non-binary format that can be easily parsed by most programming languages.

Beyond the HD map and object states, the dataset includes a geo-referenced and anonymized example picture taken from the drone perspective of each intersection i. This picture both provides a way of visualizing the trajectory data, as well as a supplementary input to the provided HD map.

A. Dataset Statistics

The dataset was recorded at different times of day, for each roundabout including at least 2 h at the rush hour times in the morning and afternoon, as well as regular intervals in between rush hours.

The dataset spans 62.7 h, of which 18.8 h cover the first roundabout rdb_1 and the remaining 43.9 h are distributed among the remaining six roundabouts rdb_2 to rdb_7, with varying lengths around 7 h for each. An example picture of each roundabout is depicted in Fig. 2. In total 84,774 trajectories are included in the dataset, covering 8,501.14 km. A detailed overview of the `openDD` dataset, distinguishing between the seven different roundabouts included in the dataset, is provided in Table II. Here, the number of trajectories, the average trajectory duration, length, velocity, and total acceleration is stated for each object class, as well as for each roundabout. The average trajectory duration over all classes and all data subsets is 17.64 s, with an average trajectory length of 100.28 m.

The average velocity is 6.63 m/s and the average total acceleration is $1.42\,\text{m/s}^2$.

The relatively high amount of vehicles, 81,372 across the whole dataset, compared to the 3,402 pedestrians and bicyclists, is caused by the high percentage of covered rush hour times, as well as the remote locations of some of the covered roundabouts. The roundabout rdb_6 has an especially high traffic load with 13,644 unique vehicles passing the roundabout in 6.9 h.

Roundabout rdb_2 has a very high average trajectory duration of pedestrians, with 65.42 s compared to the average pedestrian trajectory duration of 87.64 s. The high pedestrian trajectory duration of rdb_2 is caused by several pedestrians idling in the recordings of rdb_2.

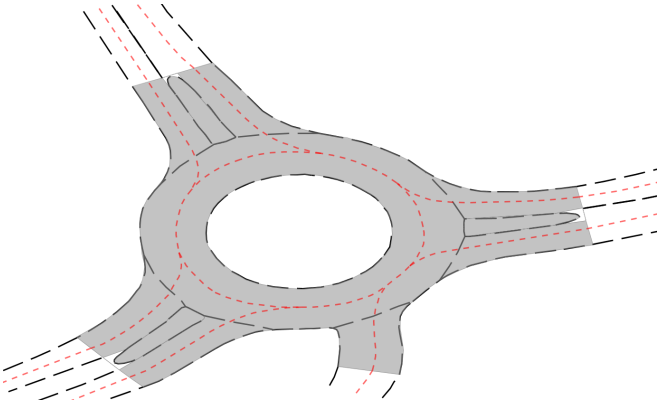

Fig. 3: An exemplary visualisation of the shapefile for rdb_1 included in the dataset, created by the open source geographic information system (GIS) `OpenJUMP`. The centerlines are decoded in red dashed lines, whereas the lane boundaries are drawn in black dashed lines. The grey surface visualizes the polygon marked as *drivable area*.

IV. Using the Dataset

Publications of trajectory prediction models that use this dataset should be evaluated in a uniform fashion. To this end we define metrics to evaluate predicted trajectories, different splits of the `openDD` dataset, and propose several challenges using this dataset in the following.

A. Distance Metrics

Similar to our previous work [3], we define several distance metrics $D\big(\mathcal{T}^{(j)}, \bar{\mathcal{T}}^{(j)}\big)$ that can be used to evaluate the accuracy of a trajectory prediction algorithm. For a given object with index j, this distance metric D compares the predicted trajectory $\mathcal{T}^{(j)}$ with the actual ground truth trajectory $\bar{\mathcal{T}}^{(j)}$ of the object, as given in the dataset. In the example scripts that are made available with the dataset, implementations of the used metrics are provided.

Euclidean displacement at time t_n: The Euclidean point-to-point distance between the n-th trajectory point of $\mathcal{T}^{(j)}$ and the m-th trajectory point of $\bar{\mathcal{T}}^{(j)}$ is defined as

$$\begin{aligned} &D_{\text{Et}}\Big(\mathcal{T}^{(j)}(n), \bar{\mathcal{T}}^{(j)}(m)\Big) \\ &\quad = \sqrt{\Big(x_n^{(j)} - \bar{x}_m^{(j)}\Big)^2 + \Big(y_n^{(j)} - \bar{y}_m^{(j)}\Big)^2}. \end{aligned} \tag{2}$$

Mean-squared Euclidean distance: Given two trajectories $\mathcal{T}^{(j)}, \bar{\mathcal{T}}^{(j)}$, spanning the same sequence of time instants $n \in \mathcal{N} = \{0, 1, \ldots, N-1\}$, the mean squared Euclidean distances *between the two entire trajectories* is defined as the normalized sum of the squared Euclidean distances between the points corresponding to the same time instant n:

$$\begin{aligned} &D_{\text{MSE}}\Big(\mathcal{T}^{(j)}, \bar{\mathcal{T}}^{(j)}\Big) \\ &\quad = \frac{1}{N} \sum_{n \in \mathcal{N}} D_{\text{Et}}^2\Big(\mathcal{T}^{(j)}(n), \bar{\mathcal{T}}^{(j)}(n)\Big). \end{aligned} \tag{3}$$

TABLE II: Statistics of the `openDD` dataset, distinguishing the seven included roundabouts.

Data Subset	rdb_1	rdb_2	rdb_3	rdb_4	rdb_5	rdb_6	rdb_7	all
Recorded time	18.8 h	7.5 h	7.0 h	7.7 h	7.1 h	6.9 h	7.7 h	62.7 h
# drone flights	153	56	54	69	60	52	57	499
# trajectories								
passenger **c**ars	26,879	7,685	7,100	5,983	3,510	11,730	6,512	69,399
van	2,630	740	676	497	396	923	782	6,644
truck	347	420	311	79	88	484	394	2,123
bus	551	79	61	76	38	78	49	932
pedestrian	963	16	38	50	122	607	23	1,819
t**r**ailer	529	367	240	71	81	393	332	2,013
motorcycle	143	11	14	32	9	36	16	261
bi**y**clist	831	52	119	96	123	332	30	1,583
	32,873	9,370	8,559	6,884	4,367	14,583	8,138	84,774
Average trajectory duration								
passenger **c**ars	18.05 s	16.01 s	12.69 s	15.74 s	11.97 s	18.54 s	13.96 s	16.47 s
van	17.25 s	16.43 s	12.38 s	16.16 s	12.52 s	18.62 s	14.45 s	16.16 s
truck	17.67 s	17.97 s	11.58 s	18.40 s	14.75 s	16.80 s	17.21 s	16.46 s
bus	17.44 s	17.44 s	16.76 s	21.45 s	12.70 s	16.58 s	14.75 s	17.32 s
pedestrian	63.69 s	82.17 s	76.76 s	73.13 s	50.66 s	70.24 s	41.80 s	65.42 s
t**r**ailer	17.79 s	18.27 s	11.86 s	17.82 s	13.91 s	17.38 s	16.90 s	16.79 s
motorcycle	16.89 s	14.35 s	17.51 s	15.35 s	12.10 s	16.76 s	12.51 s	16.18 s
bi**y**clist	23.13 s	19.84 s	24.70 s	22.07 s	21.50 s	26.68 s	18.00 s	23.60 s
	19.43 s	16.37 s	13.09 s	16.39 s	13.47 s	20.78 s	14.38 s	17.64 s
Average trajectory length								
passenger **c**ars	96.17 m	120.77 m	80.76 m	111.55 m	92.83 m	108.81 m	108.27 m	101.75 m
van	93.29 m	120.21 m	77.60 m	109.65 m	93.34 m	106.53 m	107.69 m	99.45 m
truck	86.66 m	104.42 m	59.28 m	108.42 m	91.54 m	87.24 m	105.98 m	90.89 m
bus	84.20 m	106.05 m	78.16 m	106.27 m	67.09 m	81.70 m	83.46 m	86.51 m
pedestrian	71.24 m	110.24 m	96.12 m	90.33 m	65.77 m	101.00 m	75.65 m	82.25 m
t**r**ailer	84.34 m	103.96 m	57.86 m	99.54 m	82.74 m	86.33 m	103.38 m	88.76 m
motorcycle	93.09 m	128.27 m	90.62 m	105.43 m	93.83 m	96.49 m	107.03 m	97.30 m
bi**y**clist	97.30 m	97.75 m	97.39 m	94.95 m	81.13 m	99.43 m	81.14 m	96.06 m
	94.74 m	119.08 m	79.38 m	110.78 m	91.36 m	106.63 m	107.56 m	100.28 m
Average velocity								
passenger **c**ars	6.00 m/s	8.13 m/s	6.88 m/s	7.37 m/s	8.03 m/s	6.66 m/s	8.25 m/s	6.87 m/s
van	6.03 m/s	7.83 m/s	6.69 m/s	6.97 m/s	7.69 m/s	6.27 m/s	7.83 m/s	6.71 m/s
truck	5.39 m/s	6.36 m/s	5.33 m/s	6.09 m/s	6.41 m/s	6.25 m/s	6.47 m/s	6.04 m/s
bus	5.28 m/s	6.48 m/s	5.06 m/s	5.34 m/s	5.62 m/s	5.26 m/s	5.79 m/s	5.41 m/s
pedestrian	1.27 m/s	1.85 m/s	1.38 m/s	1.56 m/s	1.39 m/s	1.47 m/s	1.96 m/s	1.37 m/s
t**r**ailer	5.32 m/s	6.22 m/s	5.09 m/s	5.94 m/s	6.30 m/s	6.05 m/s	6.53 m/s	5.86 m/s
motorcycle	5.93 m/s	9.19 m/s	6.26 m/s	7.09 m/s	7.90 m/s	6.57 m/s	9.11 m/s	6.58 m/s
bi**y**clist	4.64 m/s	5.32 m/s	4.30 m/s	4.70 m/s	4.15 m/s	4.09 m/s	5.02 m/s	4.50 m/s
	5.80 m/s	7.91 m/s	6.69 m/s	7.21 m/s	7.62 m/s	6.33 m/s	8.01 m/s	6.63 m/s
Average acceleration								
passenger **c**ars	1.16 m/s^2	1.73 m/s^2	1.57 m/s^2	1.75 m/s^2	1.78 m/s^2	1.65 m/s^2	1.82 m/s^2	1.49 m/s^2
van	1.09 m/s^2	1.60 m/s^2	1.42 m/s^2	1.63 m/s^2	1.61 m/s^2	1.46 m/s^2	1.61 m/s^2	1.37 m/s^2
truck	1.01 m/s^2	1.26 m/s^2	1.18 m/s^2	1.29 m/s^2	1.28 m/s^2	1.37 m/s^2	1.24 m/s^2	1.23 m/s^2
bus	0.87 m/s^2	1.27 m/s^2	0.98 m/s^2	0.95 m/s^2	1.07 m/s^2	1.16 m/s^2	1.22 m/s^2	0.97 m/s^2
pedestrian	0.18 m/s^2	0.30 m/s^2	0.19 m/s^2	0.24 m/s^2	0.22 m/s^2	0.21 m/s^2	0.24 m/s^2	0.20 m/s^2
t**r**ailer	0.89 m/s^2	1.25 m/s^2	1.21 m/s^2	1.23 m/s^2	1.25 m/s^2	1.39 m/s^2	1.30 m/s^2	1.18 m/s^2
motorcycle	1.01 m/s^2	1.50 m/s^2	1.18 m/s^2	1.45 m/s^2	1.45 m/s^2	1.55 m/s^2	1.91 m/s^2	1.24 m/s^2
bi**y**clist	0.60 m/s^2	0.63 m/s^2	0.77 m/s^2	0.81 m/s^2	0.78 m/s^2	0.87 m/s^2	0.71 m/s^2	0.70 m/s^2
	1.10 m/s^2	1.67 m/s^2	1.51 m/s^2	1.69 m/s^2	1.67 m/s^2	1.54 m/s^2	1.74 m/s^2	1.42 m/s^2

Modified Hausdorff (MH) distance: The following definition of the modified Hausdorff (MH) distance is adopted from a work on object matching by Dubuisson *et al.* [13].

The definition of the *point-to-set distance* between the n-th point of a trajectory $\mathcal{T}^{(j)}(n)$, and another entire trajectory $\bar{\mathcal{T}}^{(j)}$, is:

$$D_{\text{PS}}\Big(\mathcal{T}^{(j)}(n), \bar{\mathcal{T}}^{(j)}\Big) = \min_{m \in \mathcal{N}} \Big(D_{\text{Et}}\Big(\mathcal{T}^{(j)}(n), \bar{\mathcal{T}}^{(j)}(m)\Big)\Big). \tag{4}$$

The *directed modified Hausdorff* (DMH) distance is defined by Dubuisson *et al.* [13] as

$$D_{\text{DMH}}\Big(\mathcal{T}^{(j)}, \bar{\mathcal{T}}^{(j)}\Big) = \frac{1}{N} \sum_{n \in \mathcal{N}} D_{\text{PS}}\Big(\mathcal{T}^{(j)}(n), \bar{\mathcal{T}}^{(j)}\Big). \tag{5}$$

The undirected, *modified Hausdorff* (MH) distance is then computed by taking the maximum over the two directed

TABLE III: Description of the three training data splits $\mathcal{R}_1, \mathcal{R}_2, \mathcal{R}_3$, as well as of the test data splits $\mathcal{R}_A, \mathcal{R}_B, \mathcal{R}_C$, as defined for the challenges described in Section IV.

Subset	$\mathcal{R}_{123}$	$\mathcal{R}_1$		$\mathcal{R}_2$		$\mathcal{R}_3$		$\mathcal{R}_{ABC}$			
		train	val	train	val	train	val		$\mathcal{R}_A$	$\mathcal{R}_B$	$\mathcal{R}_C$
Recorded time	47.3 h	38.8 h	8.5 h	42.1 h	5.7 h	34.0 h	7.5 h	15.4 h	8.5 h	7.0 h	9.4 h
# recordings from											
rdb_1	130	107	23	0	0	107	23	23	23	0	23
rdb_2	48	40	8	40	8	40	8	8	8	0	8
rdb_3	0	0	0	0	0	0	0	54	0	54	8
rdb_4	59	49	10	49	10	49	10	10	10	0	10
rdb_5	51	42	9	42	9	42	9	9	9	0	9
rdb_6	44	36	8	36	8	0	0	8	8	0	8
rdb_7	48	39	9	39	9	39	9	9	9	0	9

distances:

$$D_{\text{MH}}\left(\mathcal{T}^{(j)}, \bar{\mathcal{T}}^{(j)}\right) = D_{\text{MH}}\left(\bar{\mathcal{T}}^{(j)}, \mathcal{T}^{(j)}\right) = \max\left(D_{\text{DMH}}\left(\mathcal{T}^{(j)}, \bar{\mathcal{T}}^{(j)}\right), D_{\text{DMH}}\left(\bar{\mathcal{T}}^{(j)}, \mathcal{T}^{(j)}\right)\right). \tag{6}$$

The MH distance captures the spatial similarity of the trajectories without considering temporal misalignments. For example, two trajectories encoding the same path traveled at different velocities would have a low MH distance, while their Euclidean displacement D_{Et} and mean squared Euclidean distance D_{MSE} would be high.

B. Dataset Splits

We divide the drone recordings of the seven roundabouts rdb_i into subsets for training, validation, and testing, as specified in Table III. The exact assignment of recordings to the different subsets introduced in the following, defining which recording belongs to which subset, is provided in the dataset.

For testing purposes, we use all recordings r from rdb_3, as well as 15% of the recordings from the other roundabouts making up the total test set $\mathcal{R}_{ABC} \subset \mathcal{R}$. We define three different subsets of the total test set $\mathcal{R}_{ABC}$ to evaluate algorithms on: $\mathcal{R}_A$, $\mathcal{R}_B$, $\mathcal{R}_C \subset \mathcal{R}_{ABC}$.

The subset $\mathcal{R}_A$ includes all recordings in $\mathcal{R}_{ABC}$, but the ones of rdb_3, thus it includes 15% from all roundabouts rdb_i with $i \in \{1, 2, 4, 5, 6, 7\}$. The second subset $\mathcal{R}_B$ covers all recordings of rdb_3. Lastly, $\mathcal{R}_C$ includes 15% from the recordings of rdb_3, as well as all recordings from the other roundabouts included in $\mathcal{R}_{ABC}$, such that in total 15% of each roundabout are covered by this test set.

For training purposes, from the entire data $\mathcal{R} = \mathcal{R}_{ABC} \cup \mathcal{R}_{123}$ we split the recordings $\mathcal{R}_{123}$ not included in $\mathcal{R}_{ABC}$ into three different splits $\mathcal{R}_k = \mathcal{R}_k^{\text{train}} \cup \mathcal{R}_k^{\text{val}}, k \in \{1, 2, 3\}$. To define the splits $\mathcal{R}_k$, we split the data included in $\mathcal{R}_{123}$ for the roundabouts $\text{rdb}_i, i \in \{1, 2, 4, 5, 6, 7\}$, such that around 18% of the recordings of each roundabout, except rdb_3, form the validation set and the remaining 82% the training set. For the first split $\mathcal{R}_1$ we include the training and validation subsets formed in this way for all the roundabouts included in $\mathcal{R}_{123}$. The second split $\mathcal{R}_2$, and third split $\mathcal{R}_3$ are equal to $\mathcal{R}_1$, but leave out all recordings from rdb_1 and rdb_6, respectively.

An important feature of this proposed division of the dataset is that the splits $\mathcal{R}_k$ can be combined with any of the test sets $\mathcal{R}_A, \mathcal{R}_B$, and $\mathcal{R}_C$ to analyze different aspects of the learning process. The test set $\mathcal{R}_A$ only includes recordings for topologies that are also included in $\mathcal{R}_{123}$, allowing for an evaluation of the model's ability to predict trajectories for previously seen roundabout topologies. The test set $\mathcal{R}_B$ includes only recordings from an unseen roundabout, thus it is suitable to evaluate the generalization capability of the learned model. Especially a combination with the split $\mathcal{R}_3$ is of interest, since $\mathcal{R}_3$ does not include the data of rdb_6, which is the only other roundabout with a similar topology including lanes to skip the center roundabout lane. Lastly, the test set $\mathcal{R}_C$ is a mixture between the other two test sets, enabling an evaluation of both the learning capacity of the model, as well as its generalization ability.

C. Challenges

We encourage all publications using the `openDD` dataset to report their results using the Euclidean displacement as defined in (3), and the MH as defined in (7) at the maximal prediction horizon they are reporting, and after 1 s, 3 s, and 6 s, if applicable.

Along the lines of our previous work [3], we propose to investigate the utility of the various information of the environment provided in the dataset. Thus, we invite parties interested in using the dataset to adopt their algorithms for trajectory prediction in such a way that they can work with variable input data.

Out of the possible nine combinations between the three test sets $\mathcal{R}_A, \mathcal{R}_B$, and $\mathcal{R}_C$ and the training and validation splits $\mathcal{R}_K$, we encourage researchers using the dataset to report the results of the following four combinations, with the first two being the most relevant.

Train on $\mathcal{R}_1$, test on $\mathcal{R}_A$: All roundabout topologies tested upon have been seen during the training. Thus the results on this combination will measure the general capability of the model to solve the task at hand.

Train on $\mathcal{R}_1$, test on $\mathcal{R}_B$: The test set only includes data covering a previously unseen roundabout, this combination can be used to assess the generalization capability of the evaluated model.

Train on $\mathcal{R}_3$, test on $\mathcal{R}_B$: Only recordings from a previously unseen roundabout, rdb_3 are included in the test set. Additionally, no recordings from the roundabout with the road topology most similar to the one of the test roundabout, rdb_6 is included in $\mathcal{R}_3$. This combination represents an even more difficult generalization evaluation.

Train on $\mathcal{R}_2$, test on $\mathcal{R}_C$: No recordings from rdb_1, the roundabout which covers almost 20 h, is included in $\mathcal{R}_2$. Recordings from both seen and unseen roundabouts is included in the test set. This allows for an evaluation of both the capability of the model as well as the generalization ability and has an almost balanced amount of hours covered for each roundabout in $\mathcal{R}_1$.

Beyond the reporting of the aforementioned measures and training/testing splits, we propose three further research challenges for trajectory prediction using the `openDD` dataset:

1) Evaluation of the benefit of knowledge of the movement of other objects up to time instant t.
2) Evaluation of the benefit of the provided map data, divided by centerlines, lane boundaries and drivable areas. Here, a separate evaluation with the same algorithm using all of the provided information, only centerlines, and only drivable areas is desirable.
3) Given the image of each intersection $i \in \{1, \ldots, I\}$ provided in the dataset is used by the trajectory prediction algorithm, we would like the authors to evaluate the benefit of the image. The image can be for example used as an input for a convolutional neural network (CNN), and be combined with a birds-eye view of the current traffic scene, implicitly encoding the structure of the surroundings [3].

If challenge 3) shows that the information provided by the image gives additional benefits for the trajectory prediction task, interesting follow-up research would deal with how to integrate this information into the HD map.

V. FUTURE WORK

The `openDD` dataset introduced in this work is the biggest published trajectory dataset recorded from a drone perspective as of today. In addition to its length of over 62 h, it covers varying roundabout topologies, which makes it also valuable to study the generalization of trajectory prediction algorithms trained on it. The license of the provided `openDD` dataset, covering commercial and non-commercial usage, makes it appealing to both research institutions, as well as to companies. In a future publication we plan to provide a baseline on the given dataset, addressing the challenges introduced in Section IV.

VI. ACKNOWLEDGMENT

The authors would like to thank all partners within the H2020 co-funded project L3Pilot — grant agreement number 723051 — for their cooperation in making this dataset available online. Responsibility for the information and views set out in this publication lies entirely with the authors.

REFERENCES

[1] D. Ridel, E. Rehder, M. Lauer, C. Stiller, and D. Wolf, "A Literature Review on the Prediction of Pedestrian Behavior in Urban Scenarios," in *Proc. of ITSC*, Maui, HI, USA, Nov. 2018, pp. 3105–3112.

[2] H. Cui, V. Radosavljevic, F.-C. Chou, T.-H. Lin, T. Nguyen, T.-K. Huang, J. Schneider, and N. Djuric, "Multimodal Trajectory Predictions for Autonomous Driving Using Deep Convolutional Networks," *arXiv:1809.10732*, Sep. 2018. [Online]. Available: http://arxiv.org/abs/1809.10732

[3] A. Breuer, S. Elflein, T. Joseph, J. Bolte, S. Homoceanu, and T. Fingscheidt, "Analysis of the Effect of Various Input Representations for LSTM-Based Trajectory Prediction," in *Proc. of ITSC*, Auckland, New Zealand, Oct. 2019, pp. 2728–2735.

[4] H. Cui, T. Nguyen, F.-C. Chou, T.-H. Lin, J. Schneider, D. Bradley, and N. Djuric, "Deep Kinematic Models for Physically Realistic Prediction of Vehicle Trajectories," *arXiv:1908.00219*, Aug. 2019. [Online]. Available: http://arxiv.org/abs/1908.00219

[5] K. Driggs-Campbell, V. Govindarajan, and R. Bajcsy, "Integrating Intuitive Driver Models in Autonomous Planning for Interactive Maneuvers," in *Proc. of ITSC*, vol. 18, Yokohama, Japan, Dec. 2017, pp. 3461–3472.

[6] "Enable-S3 Consortium." [Online]. Available: https://www.enable-s3.eu/

[7] A. Robicquet, A. Sadeghian, A. Alahi, and S. Savarese, "Learning Social Etiquette: Human Trajectory Understanding in Crowded Scenes," in *Proc. of ECCV*, Amsterdam, The Netherlands, Oct. 2016, pp. 549–565.

[8] R. Krajewski, J. Bock, L. Kloeker, and L. Eckstein, "The highD Dataset: A Drone Dataset of Naturalistic Vehicle Trajectories on German Highways for Validation of Highly Automated Driving Systems," *arXiv:1810.05642v1*, Oct. 2018. [Online]. Available: https://arxiv.org/abs/1810.05642v1

[9] D. Yang, L. Li, K. Redmill, and Ü. Özgüner, "Top-View Trajectories: A Pedestrian Dataset of Vehicle-Crowd Interaction from Controlled Experiments and Crowded Campus," in *Proc. of IV*, Paris, France, Jun. 2019, pp. 899–904.

[10] J. Bock, R. Krajewski, T. Moers, S. Runde, L. Vater, and L. Eckstein, "The inD Dataset: A Drone Dataset of Naturalistic Road User Trajectories at German Intersections," *1911.07602*, Nov. 2019. [Online]. Available: https://arxiv.org/abs/1911.07602

[11] Z. Wei, L. Sun, D. Wang, H. Shi, A. Clausse, M. Naumann, J. Kummerle, H. Konigshof, C. Stiller, A. d. L. Fortelle, and M. Tomizuka, "INTERACTION Dataset: An INTERnational, Adversarial and Cooperative moTION Dataset in Interactive Driving Scenarios With Semantic Maps," *arXiv: 1910.03088*, Sep. 2019. [Online]. Available: https://arxiv.org/abs/1910.03088

[12] F. Poggenhans, J. Pauls, J. Janosovits, S. Orf, M. Naumann, F. Kuhnt, and M. Mayr, "Lanelet2: A High-Definition Map Framework for the Future of Automated Driving," in *Proc. of ITSC*, Maui, HI, USA, Nov. 2018, pp. 1672–1679.

[13] M. Dubuisson and A. K. Jain, "A Modified Hausdorff Distance for Object Matching," in *Proc. of ICPR*, vol. 1, Jerusalem, Israel, Oct. 1994, pp. 566–568.